

Compositional Few-Shot Recognition with Primitive Discovery and Enhancing

Yixiong Zou^{1,5}, Shanghang Zhang², Ke Chen³, Yonghong Tian^{1*}, Yaowei Wang⁴, José M. F. Moura⁵
 Peking University¹, University of California, Berkeley², South China University of Technology³
 PengCheng Laboratory⁴, Carnegie Mellon University⁵
 {zoulsen,yhtian}@pku.edu.cn,shz@eecs.berkeley.edu,chenk@scut.edu.cn,wangyw@pcl.ac.cn,moura@andrew.cmu.edu

ABSTRACT

Few-shot learning (FSL) aims at recognizing novel classes given only few training samples, which still remains a great challenge for deep learning. However, humans can easily recognize novel classes with only few samples. A key component of such ability is the compositional recognition that human can perform, which has been well studied in cognitive science but is not well explored in FSL. Inspired by such capability of humans, to imitate humans' ability of learning visual primitives and composing primitives to recognize novel classes, we propose an approach to FSL to learn a feature representation composed of important primitives, which is jointly trained with two parts, i.e. primitive discovery and primitive enhancing. In primitive discovery, we focus on learning primitives related to object parts by self-supervision from the order of image splits, avoiding extra laborious annotations and alleviating the effect of semantic gaps. In primitive enhancing, inspired by current studies on the interpretability of deep networks, we provide our composition view for the FSL baseline model. To modify this model for effective composition, inspired by both mathematical deduction and biological studies (the Hebbian Learning rule and the Winner-Take-All mechanism), we propose a soft composition mechanism by enlarging the activation of important primitives while reducing that of others, so as to enhance the influence of important primitives and better utilize these primitives to compose novel classes. Extensive experiments on public benchmarks are conducted on both the few-shot image classification and video recognition tasks. Our method achieves the state-of-the-art performance on all these datasets and shows better interpretability.

CCS CONCEPTS

• **Computing methodologies** → **Computer vision**; *Image representations*; *Bio-inspired approaches*; Transfer learning.

KEYWORDS

Few-shot learning; Compositional learning; Few-shot image recognition; Few-shot video recognition; Interpretability

* indicates corresponding author.

Permission to make digital or hard copies of all or part of this work for personal or classroom use is granted without fee provided that copies are not made or distributed for profit or commercial advantage and that copies bear this notice and the full citation on the first page. Copyrights for components of this work owned by others than ACM must be honored. Abstracting with credit is permitted. To copy otherwise, or republish, to post on servers or to redistribute to lists, requires prior specific permission and/or a fee. Request permissions from permissions@acm.org.

MM '20, October 12–16, 2020, Seattle, WA, USA

© 2020 Association for Computing Machinery.

ACM ISBN 978-1-4503-7988-5/20/10...\$15.00

<https://doi.org/10.1145/3394171.3413849>

ACM Reference Format:

Yixiong Zou^{1,5}, Shanghang Zhang², Ke Chen³, Yonghong Tian^{1*}, Yaowei Wang⁴, José M. F. Moura⁵. 2020. Compositional Few-Shot Recognition with Primitive Discovery and Enhancing. In *Proceedings of the 28th ACM International Conference on Multimedia (MM '20)*, October 12–16, 2020, Seattle, WA, USA. ACM, New York, NY, USA, 10 pages. <https://doi.org/10.1145/3394171.3413849>

1 INTRODUCTION

Recently, deep learning has achieved superior performance in various tasks with sufficient labeled data. However, in practice, labels in visual recognition are expensive to obtain via manual annotation, and new classes of objects may arise dynamically in nature. Therefore, it is extremely difficult to annotate sufficient samples for these new classes. To address these limitations, few-shot learning (FSL) has been researched actively in recent years and recognized as a feasible solution [47], which categorizes objects from novel classes using only few training samples, with prior knowledge transferred from non-overlapping known classes that have sufficient data. However, there is still a big gap between machines and humans in the recognition ability. Humans can recognize novel classes with only few samples. As studied in cognitive science, a key component of such ability is the compositional recognition [6], which means humans can first learn primitives [26] from known classes and then compose novel concept with the learned primitives [15], as shown in Fig.1. In practice, primitives are viewed as object parts, or more broadly, components capturing the compositional structure of the examples [51]. Although known classes and novel classes are non-overlapping, they can share some primitives in common. The concept of compositional recognition has been applied in some domains such as VQA [2] and human-object interaction [29]. However, such concept has not been well explored in FSL. In this paper, to imitate humans' ability of learning primitives and utilizing primitives to compose novel classes, we propose an approach to FSL to compose novel-class samples with important primitives from known classes, which is jointly trained with two parts, i.e. primitive discovery and primitive enhancing.

In primitive discovery, we propose to use the self-supervision from object split orders to facilitate the discovery of part-related primitives and reduce the effect of semantic gaps. Specifically, as visual primitives can refer to object parts [51], the training procedure should encourage the model to recognize object parts. However, as current methods mainly rely on the supervision from image-level class labels, it may be harder to achieve this goal than that under the explicit supervision of object parts. Also, annotating all possible object parts is prohibitively expensive. Moreover, in the compositional recognition, transferring primitives learned on known classes to novel classes assumes they are semantically related. However,

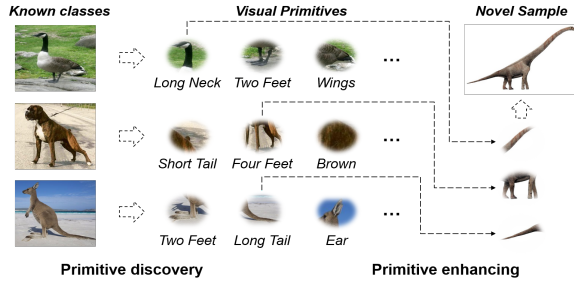


Figure 1: Human can decompose known classes into primitives and use the composition of learned primitives to recognize novel samples. To imitate this ability, we propose an approach to few-shot recognition to learn a feature representation composed of important primitives, which is jointly trained with primitive discovery and primitive enhancing.

various classes with different semantic gaps may exist in novel classes. Therefore, to assist the discovery of part-related primitives without laborious annotations and reduce the effect of semantic gaps, we propose to use the self-supervision from object split orders to assist the learning procedure. Specifically, we split the input image horizontally and vertically, perm the splits, and ask the model to recognize which perms are applied to them. As the splitting operation tends to break the entire object into parts, the model is encouraged to recognize splits by recognizing parts, thus discovering primitives and latently encoding them in the network. Moreover, as objects with relatively large semantic gaps may share similar structures (e.g., the upper and lower parts of dogs and cars can be easily distinguished, although they are not highly semantically related), self-supervision from object structures [31, 42] may help to alleviate the influence of semantic gaps. As the supervision from class labels still dominates the training, primitives other than object parts will not be sacrificed.

In primitive enhancing, we propose the soft composition mechanism with an Enlarging-Reducing loss (ER loss) to compose novel-class samples with the discovered primitives and enhance the influence of important primitives. Specifically, our method is based on the widely adopted baseline model [8, 23, 35, 46, 48, 51], which first conducts known-class classification with deep networks, then utilizes the trained network to extract feature for novel-class samples, and finally performs the Nearest Neighbor classification. Current works [5, 16, 59] on the deep networks’ interpretability show that channels in the penultimate layer of deep networks can correspond to some certain patterns (e.g., texture, object parts) in the input sample. Inspired by these works, we propose the soft composition mechanism based on the *compositional view* which regards each channel of the penultimate layer as a primitive. During known-class training, the classification probability of the input can be treated as the normalized weighted sum of the activation on primitives, where the weights of primitives are represented in the fully connected (FC) layer’s parameters. During novel-class testing, as all channels are already contained in the extracted novel-class feature, the cosine-similarity-based Nearest Neighbor classification can be viewed as comparing two primitive sets and outputting an overall similarity score. Since the novel-class composition of the baseline model suffers from the problem that all primitives are averagely weighted, which harms the composition by the influence from those trivial

primitives, a straightforward solution may be the hard composition mechanism, which explicitly select all the important primitives and neglect those trivial ones. However, such mechanism may require to modify the network structure to allow a dynamic number of primitives, which is complicated and difficult to implement. Therefore, to both achieve effective composition and simplify the hard composition mechanism, we design the soft composition mechanism with the ER loss, which enhances the influence of important primitives. With higher influence from these important primitives, the unknown-class features can be better composed. The proposed ER loss is inspired both mathematically and biologically. Mathematically, important primitives in known-class recognition should have larger influence on novel-class recognition. Therefore, we first define the influence of primitives in the novel-class classification. Then by deduction, we find that the influence of those important primitives can be enhanced by enlarging the activation of them while reducing that of others during the known-class training, leading to the proposed ER loss. Biologically, as each primitive is weighted by the parameter (neuron) in the FC layer connected to it, this primitive-neuron pair can be viewed as two connected cells. As empirically highly-activated FC neurons are always connected to highly-activated primitives, according to the biologically widely observed Hebbian Learning rule [25], we enlarge the activation of the connected primitives, which can be implemented as the enlarging term of the ER loss. Moreover, as primitives can be viewed as competing with each other to get a higher importance during known-class training, according to the Winner-Take-All (WTA) mechanism [13] in human cortex, we reduce the activation of the losers’ activation, which can be implemented as the reducing term of the ER loss. Although the ER loss is simple, it is biologically interpretable and empirically effective, and requires no extra parameters or modifications to the network structure. Moreover, combining with the compositional view, we can then explain which primitives from known classes compose the given novel sample by the feature map visualization, showing better interpretability for the deep-learning-based FSL. After the above training on known classes, the trained network will be used to extract features and perform Nearest Neighbor classification on novel classes.

Compared with current works, our model has better interpretability due to both the compositional recognition (as validated in section 4.3) and the biological interpretation of the ER loss (as stated in section 3.3.2). The most relevant work with ours is [51], which pushes the visual feature close to the sum of human annotated attributes. Compared with it, our method differs in (1) we don’t need human annotated attributes, (2) instead of feature vectors, we treat channels within a single feature layer as the visual primitives, and the composition is achieved in the channel level instead of the feature level (summing feature vectors), (3) our model is easier to be jointly trained in an end-to-end manner, while [51] points out that for easier converging, it must adopt a two-stage training strategy.

In all, our contributions can be summarized as follows.

- Inspired by humans’ compositional recognition, we propose an approach to FSL to learn a feature representation composed of important primitives, which is jointly trained with primitive discovery and primitive enhancing.
- To facilitate the discovery of part-related primitives without laborious annotations and reduce the effect of semantic gaps,

in primitive discovery, we propose to use the self-supervision from object split orders to assist the primitive learning.

- To compose the novel-class feature, in primitive enhancing, we provide our compositional view for the FSL baseline model. To modify this model for effective composition, inspired both mathematically and biologically (the Hebbian learning rule and the WTA mechanism), we propose a soft composition mechanism by enlarging the activation of important primitives while reducing that of others (ER loss).
- Extensive experiments on three popular benchmarks demonstrate better interpretability and superior performance of the proposed method compared to the state-of-the-arts on both few-shot image and video recognition tasks.

2 RELATED WORK

Few-shot learning (FSL) methods can typically be grouped into meta learning based methods, metric learning based methods, and data augmentation based methods. The meta-learning based methods develop a meta-learner model that can quickly adapt to a new task given a few training examples [3, 14, 22, 34, 41, 47, 58]. Typical works include learning model initializations [14], learning the stochastic gradient descent optimizer [47] and learning the weight-update mechanism with an external memory [41]. The embedding and metric learning based methods address the FSL problem by learning the feature representations that preserve the class neighborhood structure and comparing samples [17, 32, 38, 49, 53, 56]. The data augmentation based methods solve the FSL problem by augmenting the training data using prior knowledge, such as learning a data generator to hallucinate novel-class data [23, 55]. However, they mainly treat each class as a whole, while we decompose them into primitives and operate on the primitive level to select and enhance the most effective ones, leading to a better interpretability.

Compositional recognition is the recognition by primitives, and has been well studied in the cognitive science [6, 15, 26]. This concept has been applied to some domains: [40] points that the model will benefit from compositional learning of visual tasks to have better generalization to novel tasks. [29] proposes to decompose human-object interaction into action and object. [44] decomposes complex attributes into simple ones, and learns their compositions for zero-shot learning. Very recently [51] proposes to push the visual feature close to the combination of attribute embedded features, decomposing the visual feature into manual labeled attributes. However, this concept is still far from being well explored in FSL. All these methods largely rely on human annotated attributes/database (e.g. CUB [54] attributes used in [51]), which is expensive. Compared with them, our method is able to learn without laborious annotations, and can be easily trained in an end-to-end manner.

Interpretability of deep networks has been studied in many aspects [5, 16, 59], showing that channels in the penultimate layer of deep networks correspond to some certain patterns in the input images. These patterns may include color, texture, object, etc [5]. In this work, inspired by these studies, we view each channel as a primitive, and developed a soft composition mechanism to compose novel-class features by learned primitives.

Self-supervised learning aims at learning from the supervision of the object structure, alleviating the need of supervision from manual

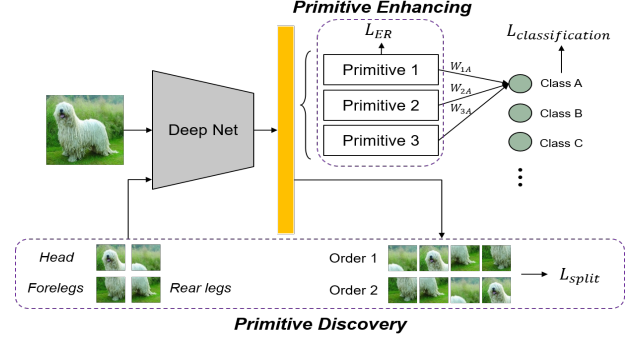


Figure 2: Framework. A self-supervised loss based on the split order prediction is applied to discover part-related primitives and alleviate the effect of semantic gaps. To better utilize learned primitives to compose novel classes, a soft composition mechanism is proposed, which is achieved by the math- and bio-inspired ER loss to enlarge the activation of important primitives while reducing that of others.

labels, and has been researched in the field of unsupervised/semi-supervised learning [31, 42]. Recently, this mechanism is also applied in FSL by methods such as predicting the rotation [19, 37] and predicting the relative position [19]. In this work, inspired by these previous works, we propose to use the self-supervised split loss to learn part-related primitives and alleviate the influence of the semantic gap between known and novel classes.

3 METHODOLOGY

In this section, the proposed method aims to imitate humans’ compositional recognition, and is jointly trained with primitive discovery and primitive enhancing. A self-supervised split loss is applied to discover the primitives related to object parts without laborious annotations and alleviate the effect of semantic gaps. To compose novel classes with learned primitives, we provide our compositional view for the FSL baseline model. To modify this model for effective composition, a soft composition mechanism is proposed, which is achieved by the math- and bio-inspired Enlarging-Reducing (ER) loss to enlarge the activation of important primitives while reducing that of others. The framework is shown in Fig.2. The network is trained on known classes, and then the Nearest Neighbor classification is performed on novel classes.

3.1 FSL baseline model

Following the setting of current works [47, 53], we are provided with a large-scale known set \mathcal{D}_{known} with known classes C_{known} and a novel/unknown¹ set $\mathcal{D}_{unknown}$ with unknown classes $C_{unknown}$. Note that $C_{known} \cap C_{unknown} = \emptyset$. Few-shot learning aims at recognizing query samples from unknown classes given only few (1 to 5) training samples. Specifically, from $\mathcal{D}_{unknown}$, small datasets (a.k.a episode/task) with individual training set and query set will be sampled. In each episode, the training set (a.k.a support set) contains K classes $\{C_i^U\}_{i=1}^K \subset C_{unknown}$ and N samples $\{x_{ij}^U\}_{j=1}^N$ in each class C_i^U (i.e. K -way N -shot), and the query set contains a query sample x_q from $\{C_i^U\}_{i=1}^K$. The non-parametric testing on

¹ Novel class is equivalent to Unknown class.

each novel-class episode is based on the Nearest-Neighbor classification. The probability that x_q belongs to class i is represented as

$$P(y_i|x_q) = \frac{\exp(s(f_\theta(x_q), p_i^U))}{\sum_{k=1}^K \exp(s(f_\theta(x_q), p_k^U))} \quad (1)$$

where $f_\theta()$ is the network with parameter θ , $p_i^U = \frac{1}{N} \sum_{j=1}^N f_\theta(x_{ij}^U)$ is the prototype of the class C_i^U , and $s(\cdot)$ is a similarity function (cosine similarity). The averaged performance on the episodes sampled from $\mathcal{D}_{unknown}$ will be the final performance of the model.

To enable the model of the novel-class Nearest-Neighbor classification, the known-class training must provide a feature extractor in the embedding space. While training on \mathcal{C}_{known} , simply training a classifier (CNN backbone + fully connected (FC) classification layer) on it remains a strong baseline [8, 23, 35, 46, 48, 51]. Combined with the cosine-similarity-based novel-class classification, it can be regarded as the baseline model for FSL. In this model, the backbone CNN’s output $f_\theta(x) \in \mathbb{R}^{D \times 1}$ is regarded as the feature of the input x , and D denotes the number of channels. The forward pass of the FC layer can be represented as $W^T f_\theta(x)$, where $W \in \mathbb{R}^{D \times M}$ is the parameter of the FC layer, M denotes the number of known classes, and we follow [20, 46] to discard the bias term. In the commonly used modified version for FSL, the feature and the FC parameters are L_2 normalized [20, 46], we denote them as $f_\theta^c(x) = \frac{f_\theta(x)}{\|f_\theta(x)\|_2}$ and $W_{:,i}^c = \frac{W_{:,i}}{\|W_{:,i}\|_2}$. The classification loss is

$$L_{classification} = -\log\left(\frac{\exp(\tau W_{:,y}^{cT} f_\theta^c(x))}{\sum_{k=1}^M \exp(\tau W_{:,k}^{cT} f_\theta^c(x))}\right) \quad (2)$$

where y is the label of x , and τ is set to 30.0 following [11] which controls the peakiness of the probability distribution.

3.2 Primitive discovery

Visual primitives can refer to object parts [51]. Therefore, the primitive learning procedure should encourage the model to recognize object parts. However, current methods [49, 53] mainly rely on the image-level class labels for representation learning, which lacks the supervision for learning object parts. An alternative way is to manually label all possible object parts in each image. However, such annotation is prohibitively expensive and laborious. On the other hand, in the compositional recognition, transferring primitives learned on known classes to novel classes assumes they are semantically related. However, various classes with different semantic gaps may exist in novel classes. To facilitate the discovery of part-related primitives without laborious annotations and reduce the effect of semantic gaps, we propose to use the self-supervision from object split orders to assist primitive learning. Suppose we have an input image x to be classified (shown in Fig.2), splitting it into pieces will be likely to generate image patches containing different parts of the object in x . which encourages the model to recognize splits by recognizing parts, thus discovering primitives and latently encoding them in the network. On the other hand, as objects with relatively large semantic gaps may share similar structures (e.g., the upper and lower parts of dogs and cars can be easily distinguished, although they are not highly semantically related), self-supervision from object structures [31, 42] may help

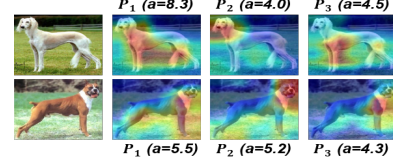


Figure 3: Primitives are shared as similar activated regions.

to alleviate the influence of semantic gaps. Therefore, inspired by current works [19, 31, 37] on self-supervised learning, we propose to use the split-based self-supervised mechanism for FSL, where we split the input image horizontally and vertically, perm the splits, and ask the model to recognize which perms are applied to them.

Specifically, given an input image x , we first divide it along rows and columns into $h \cdot v$ splits. The feature extractor will be applied to all splits to get $h \cdot v$ features, which will be denoted as $\{f_\theta(x_{rc})\}_{rc}^{h \cdot v}$, where r and c are the row id and column id respectively. We then randomly permute these splits to get a permuted sequence of splits, and ask the model to predict which permutation is applied to this sequence. This permutation-prediction task is modelled as a classification problem. Then, the permuted features are concatenated and a FC layer is applied for classification. However, if the number of splits is large, there will be $(h \cdot v)!$ orders, and classifying the permuted sequence into all these classes will be difficult. To solve this problem, M^s permutations with max Hamming distances [42] are used to permute the pieces. Denoting the concatenated feature vector as $f^s \in \mathbb{R}^{h \cdot v \cdot D}$, the loss is calculated as

$$L_{split} = -\log(P(y^s|f^s)) \quad (3)$$

where y^s is the permutation label of f^s . Note that although the part-related primitives are strengthened, other kinds of primitives are not sacrificed, because the classification loss in equation 2 still dominates the training process.

3.3 Primitive enhancing

Assume we have well-trained primitives, the next step is to compose novel classes. To achieve this goal, we must first know how primitives are represented in the deep network. Below we first provide our compositional view of the FSL baseline model with inspirations from current studies on the interpretability of deep networks, and then introduce our proposed composition mechanism.

Denote the feature map of $f_\theta^c(x)$ at channel j as $A_\theta(x)_j \in \mathbb{R}^{h \times w}$. Given various input x , after mapping $A_\theta(x)_j$ to the original size of the input, current studies [5, 59] on the interpretability of deep networks show that the heatmap of each channel can correspond to some certain patterns in the input. As shown in Fig. 3, we can see that (a) given the same input, the feature maps of different channels have activation on different regions (Fig. 3 rows); (b) given different inputs, the same channel has activation on similar regions with different magnitude (Fig. 3 columns). For example, given images of dogs from two classes, channel 1, 2 and 3 have activation on similar parts around chest+fore&rear legs, head, and chest+fore legs respectively with different magnitude. The phenomenon (a) means the network is capable of learning various interested regions, and these regions can be viewed to compose the whole region that the network focuses on (e.g. CAM [59]). The phenomenon (b) indicates that channels are transferable between different classes (at least to some degree). Therefore, we view each channel of $f_\theta^c(x)$ as a visual

primitive. The known-class classification probability of the input can be viewed as the normalized weighted sum of the activation on primitives, where the weights of primitives are represented in the FC layer's parameters. Then, during the novel-class testing, as all channels are already contained in the extracted novel-class feature, the Nearest Neighbor classification on novel classes can be viewed as the comparison of two primitive sets, because the calculation of the cosine similarity (i.e., L_2 normalized dot product) can be viewed as comparing the similarity on the activation of each primitive respectively, and outputting an overall similarity score.

However, as primitives are equally weighted in the novel-class feature of the baseline model, the composition may be harmed by influences from those trivial primitives. One straightforward solution may be the hard composition mechanism, which explicitly selects all important primitives and neglect those trivial ones. However, to achieve the hard composition, we must modify the network structure to allow a dynamic number of all possible primitives, which is complicated and difficult to implement. Therefore, to achieve the effective composition and simplify the hard composition, we propose a soft composition mechanism by an Enlarging-Reducing loss (ER loss) to enhance the influence of those important primitives while reducing that of others, making those important primitives nearly influence all the novel-class classification, so that the novel classes can be approximately viewed as being composed by these primitives. Compared with the hard composition mechanism, the soft composition mechanism keeps a fixed set of all candidate primitives and requires no extra modification in the baseline network structure. Moreover, combining the compositional view, we can then explain which primitives from known classes compose the given novel sample by visualizing the feature maps, which shows better interpretability for the deep-learning-based FSL (see section 4.3).

The ER loss is inspired by both mathematically and the biologically. As both inspirations give the same formulation of the adopted loss, below we first give the deduction from the mathematical view, and then the inspiration from biological studies will be included.

3.3.1 Inspiration from mathematical deduction.

In the compositional view of the FSL baseline model, primitives are transferable across classes although classes are not overlapping. As the importance of each primitive to class i is represented in $W_{:,i}^c$, we can select important primitives for each known class from the total primitive set, and the selected ones intuitively should also have higher influence in the novel-class classification.

In FSL [53], the cosine similarity function is widely adopted as the similarity function $s(\cdot)$ in equation 1. For simplicity, we handle the situation where the number of shot is 1 (i.e., $p_i^U = f_\theta(x_i^U)$). As shown in equation 1, now the similarity is computed as

$$s(f_\theta(x_q), f_\theta(x_i^U)) = \sum_{j=1}^D f_\theta^c(x_q)_j \cdot f_\theta^c(x_i^U)_j \quad (4)$$

Now we define the influence of the primitive represented by $f_\theta^c(\cdot)_k$ in novel-class classification as

$$\begin{aligned} influ^U &= \frac{f_\theta^c(x_q)_k \cdot f_\theta^c(x_i^U)_k}{s(f_\theta(x_q), f_\theta(x_i^U))} = \frac{f_\theta^c(x_q)_k \cdot f_\theta^c(x_i^U)_k}{\sum_{j=1}^D f_\theta^c(x_q)_j \cdot f_\theta^c(x_i^U)_j} \\ &= \frac{1}{(\sum_{j=1, j \neq k}^D f_\theta^c(x_q)_j \cdot f_\theta^c(x_i^U)_j) / (f_\theta^c(x_q)_k \cdot f_\theta^c(x_i^U)_k) + 1} \quad (5) \end{aligned}$$

To increase the influence of the primitive represented by $f_\theta^c(\cdot)_k$, there are two ways:

- Enlarging the term $f_\theta^c(x_q)_k \cdot f_\theta^c(x_i^U)_k$
- Reducing the term $\sum_{j=1, j \neq k}^D f_\theta^c(x_q)_j \cdot f_\theta^c(x_i^U)_j$

As primitives are shared between known classes and novel classes, we can simply achieve this goal in known-class training. To better compose novel classes with learned primitives, we propose the Enlarging-Reducing (ER) loss in known-class training as follows,

$$L_{ER} = -\lambda_1 \sum_{j \in T(W_{:,y}, D^*)} f_\theta(x)_j + \lambda_2 \sum_{j \notin T(W_{:,y}, D^*)} f_\theta(x)_j \quad (6)$$

where y is the class that the known-class sample x belongs to, and $T(D^*)$ returns the indices of top D^* elements in the given vector. Top D^* elements in $W_{:,y}$ represent the primitives that contribute the most to the classification of x to its class y . In the novel-class classification, if the primitives from $T(W_{:,y}, D^*)$ influences nearly all the similarity calculation, the novel classes can be viewed to be composed by these primitives. Relevant experiments are in Fig. 6.

Combine the primitive discovery, the total training loss is

$$L = L_{classification} + \alpha_1 L_{split} + \alpha_2 L_{ER} \quad (7)$$

where α_1, α_2 are pre-defined hyper-parameters. After training on known classes, the trained network will be used to perform Nearest-Neighbor classification on novel classes as stated in section 3.1.

3.3.2 Inspiration from biological studies.

Hebbian Learning is a widely observed unsupervised learning mechanism in human brain [25] related to memory. It is stated as when an axon of cell A is near enough to excite a cell B and repeatedly or persistently takes part in firing it, some growth process or metabolic change takes place in one or both cells such that A's efficiency, as one of the cells firing B, is increased [25]. In known-class classification, the forward pass of the FC layer (i.e. $W_{:,i}^c \top f_\theta^c(x)$) can be viewed as connected cells. Each connection is between W_{ji}^c and $f_\theta^c(x)_j$. In Fig. 5 we observe that large $f_\theta^c(x)_j$ always has large W_{ji}^c (y stands for the label of the input x) multiplied with it. As the firing of a neural cell is always observed when its membrane voltage is higher than a threshold [21], we can view W_{ji}^c and $f_\theta^c(x)_j$ as firing cells when their values are large. As large $f_\theta^c(x)_j$ is always connected with large W_{ji}^c , cells represented by them always fire together. As W_{ji}^c is easier to have a relatively larger value due to the easiness in the back propagation, according to Hebbian Learning, we increase the efficiency of $f_\theta^c(x)_j$ by enlarging its value. This mechanism can be represented by the first term in the ER loss.

Winner-Take-All mechanism is widely used in the brain cortex learning and the Spiking Neural Network [13]. It means that columns in the cortex are competing against each other, and the winner will suppress others, producing sparse spikes. While the feature extractor is being trained on known classes, each feature

channel $f_{\theta}()_j$ can be viewed as competing against each other to get larger importance in the classification, where its importance to class y is measured by W_{jy}^c . According to the Winner-Take-All mechanism, the winner should suppress all other losers, and this can be represented by the second term in the ER loss.

3.4 Auxiliary objective and regularization

As we view W as the weights for the corresponding primitive, when W is smaller, the importance of the primitive should also be lower. However, the activation of primitives can be negative (e.g., LSTM [12]), if W is also negative, the dot product will be positive, disobeying what we want. So we use $W = \text{abs}(W)$ to avoid such situation. As the weights in W are continuous and it is hard to draw a clear line between high and low, we add a sparseness loss on each column of W , which can be represented as $\frac{1}{M} \sum_{i=1}^M \|W_{:,i}\|_1$, which constrains the model to use few primitives in known-class recognition and improve the quality of each primitive, and making it easier to control the ER loss hyper-parameters. The weight for this loss is typically 0.1. To learn the object structure implicitly, we also add the self-supervised rotation loss [19, 37] to assist the learning. Given an image, it is rotated by $\{0, 90, 180, 270\}$ degrees, and the model is asked to predict which rotation is applied to the image. This self-supervised loss can also help alleviating the influence from semantic gaps. Compared with this term, our model explicitly learn primitives related to object parts by splitting images into splits.

4 EXPERIMENTS

To verify the proposed methods, we conduct extensive experiments on both few-shot image and video classification. We first introduce the datasets and implementation details. Then the comparison with state-of-the-art and the ablation study will be reported. We also visualize the primitives learned by our method, so as to provide interpretability of the proposed method. Due to the space limitation, please refer to the supplementary material for more details.

Datasets and settings. Experiments on few-shot image classification are conducted on the CUB-200-2011 (CUB) [54] and the *miniImageNet* [53] benchmarks, while experiments on few-shot video classification are conducted on the Kinetics dataset [30]. CUB contains 200 fine-grained bird classes and 11,788 images in total. Following the settings in [8, 45], we split the dataset into 100 training classes, 50 validation classes and 50 test classes. *MiniImageNet* has 100 classes selected from the ImageNet [10] with 600 images in each class, which has 64 training classes, 16 validation classes and 20 test classes. Kinetics is introduced into the few-shot video recognition task by CMN [61]. Following the provided splits, it contains 100 classes of actions with 100 videos in each class in total. We follow CMN to split the dataset into 64 training classes, 12 validation classes and 24 test classes. Following existing methods [53, 61], the mean accuracy (%) and the 95% confidence intervals of randomly generated episodes on the test (novel) sets will be reported.

Implementation details. Our model is implemented with the TensorFlow [1]. The Nesterov Momentum optimizer [50] is used with an initial learning rate of 0.01. The total training epochs on the CUB, the *miniImageNet* and the Kinetics are 57, 40 and 23, and the learning rate is dropped to 10% on (30, 40), (30, 37), (2, 19) epochs respectively. The weight decay is set to be 0.0005. Typical data augmentation methods such as random flipping and random

Table 1: Evaluative results(%) on CUB.

Method	Backbone	5-way 1-shot	5-way 5-shot
MatchingNet [53]	Conv4	61.16 \pm 0.89	72.86 \pm 0.70
ProtoNet [49]	Conv4	51.31 \pm 0.91	70.77 \pm 0.69
MAML [14]	Conv4	55.92 \pm 0.95	72.09 \pm 0.76
RelationNet [56]	Conv4	62.45 \pm 0.98	76.11 \pm 0.69
DEML+MetaSGD [60]	ResNet50	66.95 \pm 1.06	77.1 \pm 0.78
ResNet18+TriNet [9]	ResNet18	69.61 \pm 0.46	84.10 \pm 0.35
MAML++ [4]	DenseNet	67.48 \pm 1.44	83.80 \pm 0.35
SCA + MAML++ [4]	DenseNet	70.33 \pm 0.78	85.47 \pm 0.40
S2M2 [37]	ResNet18	72.40 \pm 0.34	86.22 \pm 0.53
CFA [27]	ResNet18	73.90 \pm 0.80	86.80 \pm 0.50
Cosine Classifier	ResNet18	72.22 \pm 0.33	86.41 \pm 0.18
CPDE (ours)	ResNet18	80.11 \pm 0.34	89.28 \pm 0.33

Table 2: Evaluative results(%) on the *miniImageNet*.

Method	Backbone	5-way 1-shot	5-way 5-shot
MatchingNet [53]	Conv4	46.56 \pm 0.84	55.31 \pm 0.73
ProtoNet [49]	Conv4	49.42 \pm 0.78	68.20 \pm 0.66
MAML [14]	Conv4	48.70 \pm 1.84	63.11 \pm 0.92
RelationNet [56]	Conv4	50.44 \pm 0.82	65.32 \pm 0.70
AgileNet [18]	Conv4	58.23 \pm 0.10	71.39 \pm 0.10
DEML+MetaSGD [60]	ResNet50	58.49 \pm 0.91	71.28 \pm 0.69
Dynamic FS [20]	ResNet10	55.45 \pm 0.89	70.13 \pm 0.68
SNAIL [39]	ResNet12	55.71 \pm 0.99	68.88 \pm 0.92
TADAM [43]	ResNet12	58.50 \pm 0.30	76.70 \pm 0.30
Acti (<i>trainval</i>) [46]	WRN-28-10	59.60 \pm 0.41	73.74 \pm 0.19
LEO (<i>trainval</i>) [48]	WRN-28-10	61.76 \pm 0.08	77.59 \pm 0.12
DCO [33]	ResNet12	62.62 \pm 0.61	78.63 \pm 0.46
DCO (<i>trainval</i>) [33]	ResNet12	64.09 \pm 0.62	80.00 \pm 0.45
CTM [36]	ResNet18	64.12 \pm 0.82	80.51 \pm 0.13
Cosine Classifier	ResNet10	55.97 \pm 0.26	74.95 \pm 0.24
Ours	ResNet10	62.66 \pm 0.69	77.45 \pm 0.71
Ours (<i>trainval</i>)	ResNet10	64.37 \pm 0.77	79.10 \pm 0.74
Cosine Classifier	ResNet12	56.26 \pm 0.28	74.97 \pm 0.24
Ours	ResNet12	63.21 \pm 0.78	79.68 \pm 0.82
Ours (<i>trainval</i>)	ResNet12	64.17 \pm 0.84	80.47 \pm 0.89
Cosine Classifier	ResNet18	56.92 \pm 0.28	75.39 \pm 0.24
Ours	ResNet18	64.44 \pm 0.79	79.06 \pm 0.57
Ours (<i>trainval</i>)	ResNet18	65.55 \pm 0.72	80.66 \pm 0.75

Table 3: Evaluation(%) on 5-way few-shot action recognition.

Method	5-way 1-shot	5-way 5-shot
RGB w/o mem	28.7	48.6
Flow w/o mem	24.4	33.1
LSTM(RGB) w/o mem	28.9	49.0
Nearest-finetune	48.2	62.6
Nearest-pretrain	51.1	68.9
Matching Network [53]	53.3	74.6
MAML [14]	54.2	75.3
Plain CMN [28]	57.3	76.0
LSTM-cmb	57.6	76.2
CMN [61]	60.5	78.9
TARN [7]	66.55	80.66
Cosine classifier	67.05 \pm 0.72	80.00 \pm 0.59
CPDE (ours)	69.14 \pm 0.68	82.19 \pm 0.60

brightness are adopted. In L_{split} , the rows and columns are set to 2, the weight α_1 is set to 0.5 for all datasets. In L_{ER} , the weight λ_1 is set to 1.0 and λ_2 is set to 0.5, and D^* is set to 5. The overall weight α_2 is set to 0.1. Hyper-parameters are chosen on the validation set.

4.1 Comparison with state-of-the-art

Comparative evaluation with existing algorithms on few-shot image recognition can be illustrated in Tables 1, 2, 3 and 4. We denote our baseline model as the Cosine Classifier. On the CUB dataset, we follow the same data pre-processing as [45, 52, 57] to use the available bounding boxes to crop the images. On the *miniImageNet*, we follow [33, 46, 48] to train the model using the training set with (*trainval*) and without the validation set. In Tables 1 and 2, our

Table 4: Top-5 accuracy(%) for the 100-way classification task on CUB. Note that in CompCos, attribute annotations are used. We can achieve comparable (even slightly better in 1-shot) performance *without such annotations*.

Method	100-way 1-shot	100-way 2-shot	100-way 5-shot
ProtoNet [49]	43.2	54.3	67.8
MatchingNet [53]	48.5	57.3	69.2
RelationNet [56]	39.5	54.1	67.1
CompCos [51]	53.6	64.8	74.6
Cosine Classifier	48.22 \pm 0.38	60.79 \pm 0.43	72.81 \pm 0.39
CPDE (ours)	54.01 \pm 0.56	64.73 \pm 0.51	74.14 \pm 0.41

Table 5: Ablation study of each module.

Study Case	Method	5-way 1-shot (%)	5-way 5-shot (%)
CUB ResNet18	cosine classifier	72.22 \pm 0.33	86.41 \pm 0.18
	+ auxiliary terms	74.14 \pm 0.33	87.49 \pm 0.48
	+ L_{split}	76.10 \pm 0.37	88.09 \pm 0.24
	+ L_{ER}	80.11 \pm 0.34	89.28 \pm 0.33
<i>mini</i> ImageNet ResNet10	cosine classifier	55.97 \pm 0.26	74.95 \pm 0.24
	+ auxiliary terms	58.35 \pm 0.26	76.16 \pm 0.56
	+ L_{split}	59.96 \pm 0.29	76.51 \pm 0.25
	+ L_{ER}	62.66 \pm 0.69	77.45 \pm 0.71
Kinetics ResNet50	cosine classifier	67.05 \pm 0.72	80.00 \pm 0.59
	+ auxiliary terms	67.84 \pm 0.53	80.68 \pm 0.61
	+ L_{ER}	69.14 \pm 0.68	82.19 \pm 0.60

method can achieve significantly better performance than existing methods in both 5-way 1-shot and 5-way 5-shot tasks. For few-shot action classification, we follow [61] to adopt the ResNet50 [24] as our backbone and pre-train it on the ImageNet. To capture the temporal information, we add a 1-layer LSTM [12] with 512 units on the top of the ResNet50, and the split loss and the rotation loss are not applied. We averagely sample 5 RGB frames from each video. Similarly, superior performance of our method to the state-of-the-art methods can be observed in Table 3. To compare with the compositional method CompCos [51] fairly, we follow them to use the ResNet10 [24] backbone, and split the CUB dataset to 100 known classes and 100 novel classes. The evaluation are carried on the 100-way classification of the novel classes in Table 4. Note that in CompCos, attribute annotations are used, while in our method, **we do not use such annotations** but achieve comparable performance (even slightly better in 1-shot).

4.2 Ablation study

4.2.1 Verification of each module. The ablation study on the effect of different modules in (7) are shown in Table 5. The model in each line on the left hand side consists of the modules all the above and the one listed in current line. As shown in Table 5, each module is verified its rationale and positive effect on improving classification performance, especially the ER loss in the 1-shot scenario.

4.2.2 Evaluation of primitive discovery. To verify that the supervision from split orders can discover the part-related primitives, we visualized the heatmap of novel-class samples in Fig. 4. We visualize them by calculating the weighted sum of the heatmap by $\sum_{j=1}^D f(x)_j \cdot A(x)_j$ (denoted as *overall*), where all notations are the same as in the methodology. We can find that compared with the model without L_{split} , adding it can have activation on more object parts. As the primitive is encoded in each channel of the penultimate layer of deep networks, we also visualize those single channels that cover the discovered regions. This result can verify

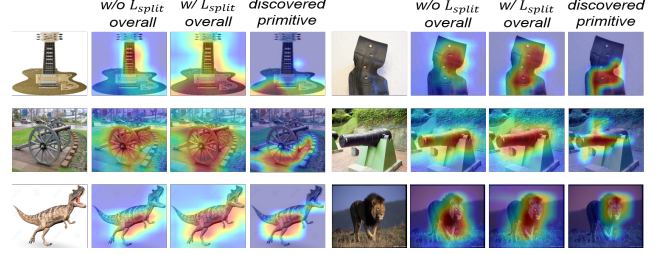


Figure 4: Heatmaps with (w/) and without (w/o) L_{split} . Images are from novel classes of *mini*ImageNet. By adding L_{split} , the model can discover more activated regions. The discovered primitive is visualized in the last column, which refers to the single channel that contains the discovered region.

that the model is pushed to extract useful information from each split, leading to the discovery of part-related primitives.

4.2.3 Evaluation of primitive enhancing. To study the effect of ER loss in primitive enhancing, we plot the distribution of weights and activation of all primitives in Fig. 5. Experiments are conducted with the ResNet10 trained on *mini*ImageNet. In Fig. 5, W is depicted with blue bars, while orange bars represent the activation on primitives. Given an input x , we first sort each channel in $W_{:,y}$ in the ascending order (y denotes the corresponding class of x), whose indices are used to sort channels in $f_\theta(x)$. We divide all channels into 32 bins (e.g. given a feature of 512 channels, there will be 16 channels in each bin), and calculate the average value of each bins to plot. All bins are divided by the max value among them for normalization. We randomly select 1000 samples from known classes and calculate the average bins. From Fig. 5, we can find that large $f_\theta(\cdot)_j$ is usually accompanied with large W_{jy} in the same feature channel, which verifies that $f_\theta^c(x)_j$ and W_{jy}^c can be viewed as connected cells firing together. By applying the auxiliary sparseness loss, in Fig. 5(middle), most weight dimensions are suppressed with relatively low values and sparse dimensions can have high response, making it easier to select the important primitives to enhance. By applying the ER loss, activation of most primitives are enforced to have lower values in Fig. 5(right) compared with Fig. 5(middle), which means enhanced influence of those important primitives achieved by the ER loss. And it is consistent with the WTA inspiration of our model.

To evaluate the effect of important primitives, we first evaluate the novel-class classification performance Acc_k of our model with top k feature channels selected by their activation (i.e. set the values in other channels to 0), whose results are shown in Fig. 6(left). Y-axis indicates the portion (%) of Acc_k credited to the performance when using all channels, i.e., Acc_k / Acc_{all} , which implies the contribution of selected primitives to the novel-class classification. As large activation tends to have large weights as shown in Fig. 5, remained primitives are more important. Compared with the baseline cosine classifier depicted with the blue curve, applying the ER loss makes important primitives have larger influence, which verifies that the novel class is better composed by important primitives.

Similarly, we then use top k large values in each column of FC parameters W to evaluate known-class classification (i.e. set values of other channels to 0 in each $W_{:,i}$), whose results are shown in

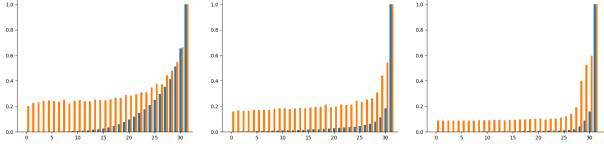


Figure 5: Ablation study on primitive enhancing. Blue and orange bars represent the distribution of $W_{:,y}$ and distribution of primitive activation, which are both sorted according to an ascending order of the values in $W_{:,y}$. Left: Cosine Classifier + $\text{abs}(W)$. Middle: + sparseness loss. Right: + ER loss.

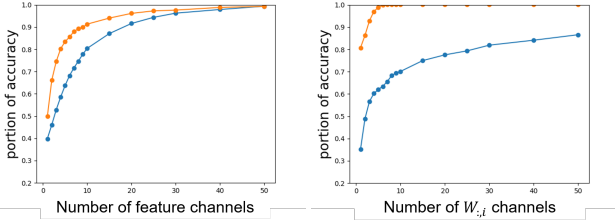


Figure 6: Left: Portion of novel-class classification accuracy maintained v.s. number of top k feature channels remained. Right: Portion of known-class classification accuracy maintained v.s. number of top k elements in $W_{:,i}$ channels remained. Our method is in orange, while the cosine classifier in blue. We can see that W can select the most important primitives, and they have larger influence in our model.

Fig. 6(right). Similarly, important primitives have larger influence in our method. Moreover, it also verifies the view that W can be treated as measuring the importance of the corresponding primitive, because only few primitives selected by W can indeed recover the total performance. Note that due to the limited data, novel classes always need more primitives to represent, thus the number of important primitives is larger in novel-class classification.

4.3 Composition of primitives

To show how novel classes are composed by primitives learned on known classes, we visualize primitives overlapped in known-class and novel novel-class classification in Fig. 7.

In Fig. 6(left), about 15 feature channels can recover 95% of classification performance, so we choose the top 15 feature channels to mark down their indices as $T(f_\theta(X^U), 15)$, where $T(a, K)$ means the set formed by top K elements' indices of the vector a . In Fig. 6(right), only 5 channels can recover the total performance. Thus we mark down their indices as $T(W_{:,i}, 5)$ for all known class i . We visualize the primitives overlapped in these two set, so that we can know which primitives in known classes compose the given novel class sample. However, as not all primitives are easy to understand, we only visualize those easy ones (most are related to object parts). As we don't have the manual annotated meaning of them, we write the possible meaning of them in the last row. The primitive/channel indices are written in the first row. \times denotes no distinguishable activation in that channel (i.e. not in $T(W_{:,i}, 5)$ or $T(f_\theta(X^U), 15)$).

Index	477	108	502	402	1	460	119
Known Classes							
	\times	\times	\times	\times	\times	\times	
	\times	\times	\times	\times	\times		\times
	\times	\times	\times	\times	\times		\times
	\times	\times	\times	\times	\times		\times
	\times	\times	\times	\times		\times	\times
	\times	\times		\times	\times	\times	\times
			\times		\times	\times	\times
Novel Classes							
	\times	\times	\times	\times	\times		
			\times	\times	\times	\times	\times
	\times				\times	\times	\times
	\times	\times		\times	\times		\times
	\times	\times	\times			\times	\times
Possible primitive name	Abdomen	Hind leg	Long body	Chest	Horse hair	Semicircle	Wheel

Figure 7: Visualization of primitives. Primitives in the same column share the channel index. Novel samples are composed of primitives learned on known classes. Most dimensions have no distinguishable activation (\times) due to the sparseness of features.

Most channels have low responses due to the sparseness of features. Known classes and last two rows of novel classes are from the *miniImageNet*. We can find that primitives in the same feature channels have high response in similar spatial regions of object parts, which are marked as red. With this visualization, for example, we can explain the dinosaur in the third row of novel classes as *having the legs and chest structure like a dog from the side view and having a neck like a fishing rod*, and explain the lion in the last row as *having chest like a dog and having horse hair like a hairy dog*.

5 CONCLUSION

We propose a novel FSL approach to imitate humans to recognize novel classes by composing primitives learned from known classes. Our method utilizes self-supervision to discover part-related primitives and alleviate the effect of semantic gaps, and enhances those important ones to better compose novel classes, which consistently achieves superior performance in few-shot image and video recognition. Moreover, the ablation study demonstrates the rationale and positive effect of each module, and reveal insights of our method via visualizing shared primitives between known and novel classes.

6 ACKNOWLEDGMENTS

This work is partially supported by grants from the National Key R&D Program of China under grant 2017YFB1002400, the National Natural Science Foundation of China under contract No. 61825101,

No. U1611461, No. 61902131), the Program for Guangdong Introducing Innovative and Entrepreneurial Teams (Grant No. 2017ZT07X183), the Fundamental Research Funds for the Central Universities (Grant No. 2019MS022), China Scholarship Council (CSC) Grant #201906010176, and grants from NVIDIA NVAIL program and the NVIDIA SaturnV DGX-1 AI supercomputer.

REFERENCES

- [1] Martín Abadi, Ashish Agarwal, Paul Barham, Eugene Brevdo, Zhifeng Chen, Craig Citro, Greg S Corrado, Andy Davis, Jeffrey Dean, Matthieu Devin, et al. 2016. Tensorflow: Large-scale machine learning on heterogeneous distributed systems. *arXiv:1603.04467* (2016).
- [2] Jacob Andreas, Marcus Rohrbach, Trevor Darrell, and Dan Klein. 2016. Learning to compose neural networks for question answering. *arXiv preprint arXiv:1601.01705* (2016).
- [3] Marcin Andrychowicz, Misha Denil, Sergio Gomez, Matthew W Hoffman, David Pfau, Tom Schaul, Brenden Shillingford, and Nando De Freitas. 2016. Learning to learn by gradient descent by gradient descent. In *NeurIPS*. 3981–3989.
- [4] Antreas Antoniou and Amos Storkey. 2019. Learning to learn by Self-Critique. *arXiv preprint arXiv:1905.10295* (2019).
- [5] David Bau, Bolei Zhou, Aditya Khosla, Aude Oliva, and Antonio Torralba. 2017. Network dissection: Quantifying interpretability of deep visual representations. In *Proceedings of the IEEE conference on computer vision and pattern recognition*. 6541–6549.
- [6] Irving Biederman. 1987. Recognition-by-components: a theory of human image understanding. *Psychological review* 94, 2 (1987), 115.
- [7] Mina Bishay, Georgios Zoumpoulis, and Ioannis Patras. 2019. TARN: Temporal Attentive Relation Network for Few-Shot and Zero-Shot Action Recognition. *arXiv preprint arXiv:1907.09021* (2019).
- [8] Wei-Yu Chen, Yen-Cheng Liu, Zsolt Kira, Yu-Chiang Frank Wang, and Jia-Bin Huang. 2019. A Closer Look at Few-shot Classification. *CoRR* abs/1904.04232 (2019). arXiv:1904.04232 <http://arxiv.org/abs/1904.04232>
- [9] Zitian Chen, Yanwei Fu, Yinda Zhang, Yu-Gang Jiang, Xiangyang Xue, and Leonid Sigal. 2018. Semantic feature augmentation in few-shot learning. *arXiv preprint arXiv:1804.05298* 86 (2018), 89.
- [10] Jia Deng, Wei Dong, Richard Socher, Li-Jia Li, Kai Li, and Li Fei-Fei. 2009. Imagenet: A large-scale hierarchical image database. In *CVPR*. Ieee, 248–255.
- [11] Jiankang Deng, Jia Guo, Niannan Xue, and Stefanos Zafeiriou. 2019. Arcface: Additive angular margin loss for deep face recognition. In *CVPR*. 4690–4699.
- [12] Jeffrey Donahue, Lisa Anne Hendricks, Sergio Guadarrama, Marcus Rohrbach, Subhashini Venugopalan, Kate Saenko, and Trevor Darrell. 2015. Long-term recurrent convolutional networks for visual recognition and description. In *CVPR*.
- [13] Rodney J Douglas and Kevan AC Martin. 2004. Neuronal circuits of the neocortex. *Annu. Rev. Neurosci.* 27 (2004), 419–451.
- [14] Chelsea Finn, Pieter Abbeel, and Sergey Levine. 2017. Model-agnostic meta-learning for fast adaptation of deep networks. *arXiv preprint arXiv:1703.03400* (2017).
- [15] Jerry A Fodor. 1975. *The language of thought*. Vol. 5. Harvard university press.
- [16] Ruth Fong and Andrea Vedaldi. 2018. Net2vec: Quantifying and explaining how concepts are encoded by filters in deep neural networks. In *Proceedings of the IEEE conference on computer vision and pattern recognition*. 8730–8738.
- [17] Victor Garcia and Joan Bruna. 2017. Few-shot learning with graph neural networks. *arXiv preprint arXiv:1711.04043* (2017).
- [18] Mohammad Ghasemzadeh, Fang Lin, Bit Darvish Rouhani, Farinaz Koushanfar, and Ke Huang. 2018. Agilenet: Lightweight dictionary-based few-shot learning. *arXiv preprint arXiv:1805.08311* (2018).
- [19] Spyros Gidaris, Andrei Bursuc, Nikos Komodakis, Patrick Pérez, and Matthieu Cord. 2019. Boosting Few-Shot Visual Learning with Self-Supervision. *arXiv preprint arXiv:1906.05186* (2019).
- [20] Spyros Gidaris and Nikos Komodakis. 2018. Dynamic Few-Shot Visual Learning without Forgetting. In *CVPR*. 4367–4375.
- [21] Xavier Glorot, Antoine Bordes, and Yoshua Bengio. 2011. Deep sparse rectifier neural networks. In *AISTATS*. 315–323.
- [22] Erin Grant, Chelsea Finn, Sergey Levine, Trevor Darrell, and Thomas Griffiths. 2018. Recasting gradient-based meta-learning as hierarchical bayes. *arXiv preprint arXiv:1801.08930* (2018).
- [23] Bharath Hariharan and Ross Girshick. 2017. Low-shot visual recognition by shrinking and hallucinating features. In *ICCV*. 3018–3027.
- [24] Kaiming He, Xiangyu Zhang, Shaoqing Ren, and Jian Sun. 2016. Deep residual learning for image recognition. In *CVPR*.
- [25] DO Hebb. 1949. Organization of behavior. New York: Wiley. (1949).
- [26] Donald D Hoffman and Whitman A Richards. 1984. Parts of recognition. *Cognition* 18, 1-3 (1984), 65–96.
- [27] Ping Hu, Ximeng Sun, Kate Saenko, and Stan Sclaroff. 2019. Weakly-supervised Compositional Feature Aggregation for Few-shot Recognition. *arXiv preprint arXiv:1906.04833* (2019).
- [28] Łukasz Kaiser, Ofir Nachum, Aurko Roy, and Samy Bengio. 2017. Learning to remember rare events. *arXiv preprint arXiv:1703.03129* (2017).
- [29] Keizo Kato, Yin Li, and Abhinav Gupta. 2018. Compositional learning for human object interaction. In *ECCV*. 234–251.
- [30] Will Kay, Joao Carreira, Karen Simonyan, Brian Zhang, Chloe Hillier, Sudheendra Vijayanarasimhan, Fabio Viola, Tim Green, Trevor Back, Paul Natsev, et al. 2017. The Kinetics Human Action Video Dataset. *arXiv:1705.06950* (2017).
- [31] Dahun Kim, Donghyeon Cho, and In So Kweon. 2019. Self-supervised video representation learning with space-time cubic puzzles. In *Proceedings of the AAAI Conference on Artificial Intelligence*, Vol. 33. 8545–8552.
- [32] Gregory Koch, Richard Zemel, and Ruslan Salakhutdinov. 2015. Siamese neural networks for one-shot image recognition. In *ICML deep learning workshop*, Vol. 2.
- [33] Kwonjoon Lee, Subhansu Maji, Avinash Ravichandran, and Stefano Soatto. 2019. Meta-learning with differentiable convex optimization. In *CVPR*. 10657–10665.
- [34] Yoonho Lee and Seungjin Choi. 2018. Gradient-based meta-learning with learned layerwise metric and subspace. *arXiv preprint arXiv:1801.05558* (2018).
- [35] Aoxue Li, Tiange Luo, Zhiwu Lu, Tao Xiang, and Liwei Wang. 2019. Large-Scale Few-Shot Learning: Knowledge Transfer With Class Hierarchy. In *CVPR*. 7212–7220.
- [36] Hongyang Li, David Eigen, Samuel Dodge, Matthew Zeiler, and Xiaogang Wang. 2019. Finding Task-Relevant Features for Few-Shot Learning by Category Transfer. In *CVPR*. 1–10.
- [37] Puneet Mangla, Mayank Singh, Abhishek Sinha, Nupur Kumari, Vineeth N Balasubramanian, and Balaji Krishnamurthy. 2019. Charting the Right Manifold: Manifold Mixup for Few-shot Learning. *arXiv preprint arXiv:1907.12087* (2019).
- [38] Thomas Mensink, Jakob Verbeek, Florent Perronnin, and Gabriela Csurka. 2012. Metric learning for large scale image classification: Generalizing to new classes at near-zero cost. In *ECCV*. Springer, 488–501.
- [39] Nikhil Mishra, Mostafa Rohaninejad, Xi Chen, and Pieter Abbeel. 2017. A simple neural attentive meta-learner. *arXiv preprint arXiv:1707.03141* (2017).
- [40] Ishan Misra, Abhinav Gupta, and Martial Hebert. 2017. From red wine to red tomato: Composition with context. In *CVPR*. 1792–1801.
- [41] Tsendsuren Munkhdalai and Hong Yu. 2017. Meta networks. In *ICML*. JMLR. org, 2554–2563.
- [42] Mehdi Noroozi and Paolo Favaro. 2016. Unsupervised learning of visual representations by solving jigsaw puzzles. In *ECCV*. Springer, 69–84.
- [43] Boris Oreshkin, Pau Rodríguez López, and Alexandre Lacoste. 2018. Tadam: Task dependent adaptive metric for improved few-shot learning. In *NeurIPS*. 721–731.
- [44] Senthil Purushwalkam, Maximilian Nickel, Abhinav Gupta, and Marc’Aurelio Ranzato. 2019. Task-Driven Modular Networks for Zero-Shot Compositional Learning. *arXiv preprint arXiv:1905.05908* (2019).
- [45] Limeng Qiao, Yemin Shi, Jia Li, Yaowei Wang, Tiejun Huang, and Yonghong Tian. 2019. Transductive Episodic-Wise Adaptive Metric for Few-Shot Learning. In *ICCV*. 3603–3612.
- [46] Siyuan Qiao, Chenxi Liu, Wei Shen, and Alan L Yuille. 2017. Few-shot image recognition by predicting parameters from activations. *CoRR*, abs/1706.03466 1 (2017).
- [47] Sachin Ravi and Hugo Larochelle. 2016. Optimization as a model for few-shot learning. (2016).
- [48] Andrei A Rusu, Dushyant Rao, Jakub Sygnowski, Oriol Vinyals, Razvan Pascanu, Simon Osindero, and Raia Hadsell. 2019. Meta-learning with latent embedding optimization. *ICLR* (2019).
- [49] Jake Snell, Kevin Swersky, and Richard Zemel. 2017. Prototypical networks for few-shot learning. In *NeurIPS*. 4077–4087.
- [50] Ilya Sutskever, James Martens, George Dahl, and Geoffrey Hinton. 2013. On the importance of initialization and momentum in deep learning. In *ICML*. 1139–1147.
- [51] Pavel Tokmakov, Yu-Xiong Wang, and Martial Hebert. 2019. Learning compositional representations for few-shot recognition. In *ICCV*. 6372–6381.
- [52] Eleni Triantafyllou, Richard Zemel, and Raquel Urtasun. 2017. Few-shot learning through an information retrieval lens. In *NeurIPS*. 2255–2265.
- [53] Oriol Vinyals, Charles Blundell, Tim Lillicrap, Daan Wierstra, et al. 2016. Matching networks for one shot learning. In *NeurIPS*.
- [54] Catherine Wah, Steve Branson, Peter Welinder, Pietro Perona, and Serge Belongie. 2011. The caltech-ucsd birds-200-2011 dataset. (2011).
- [55] Yu-Xiong Wang, Ross Girshick, Martial Hebert, and Bharath Hariharan. 2018. Low-shot learning from imaginary data. In *CVPR*. 7278–7286.
- [56] Flood Sung Yongxin Yang, Li Zhang, Tao Xiang, Philip HS Torr, and Timothy M Hospedales. 2018. Learning to compare: Relation network for few-shot learning. (2018).
- [57] Han-Jia Ye, Hexiang Hu, De-Chuan Zhan, and Fei Sha. 2018. Learning embedding adaptation for few-shot learning. *arXiv preprint arXiv:1812.03664* (2018).
- [58] Ruixiang Zhang, Tong Che, Zoubin Ghahramani, Yoshua Bengio, and Yangqiu Song. 2018. Metagan: An adversarial approach to few-shot learning. In *NeurIPS*. 2365–2374.

- [59] Bolei Zhou, Aditya Khosla, Agata Lapedriza, Aude Oliva, and Antonio Torralba. 2016. Learning deep features for discriminative localization. In *CVPR*. 2921–2929.
- [60] Fengwei Zhou, Bin Wu, and Zhenguo Li. 2018. Deep Meta-Learning: Learning to Learn in the Concept Space. *arXiv preprint arXiv:1802.03596* (2018).
- [61] Linchao Zhu and Yi Yang. 2018. Compound memory networks for few-shot video classification. In *ECCV*. 751–766.